(Received 30 October 2024, Accepted 6 December 2024, Scheduled 3 January 2025)

A Miniaturization Dual-Passband Microwave Filter Based on Load-Coupled Open Stub Lines

Xinying Sun, Chuicai Rong*, Huajie Gao, and Menglu Zhang

School of Physics and Electronic Information, Gannan Normal University, Ganzhou 341000, Jiangxi, China

ABSTRACT: In this letter, a miniaturized U-shaped microstrip filter based on a load-coupled open line is proposed. It is composed of a step impedance resonator and parallel coupled open stub line. Interfinger feed is used to enhance coupling. This configuration and coupled open stub lines form four transmission zeros between two passbands as part of open coupled stub lines to increased out-of-band rejection. The analysis of formation reason of transmission zero is conducted using lossless transmission line theory and even-odd mode analysis techniques. A filter operating at 2.53 GHz and 5.53 GHz is simulated and fabricated. The insertion loss of first passband is 1.30 dB, and return loss is -18.60 dB. The insertion loss of the second passband is 0.70 dB, and return loss is 22.89 dB. The out-of-band rejection is maintained below -20.00 dB. The final model size is $0.20\lambda_g \times 0.23\lambda_g$. The final physical measurement results confirm theoretical results.

1. INTRODUCTION

With the rapid development of wireless communication technology, high-performance, miniaturized dual-passband filters play an increasingly important role as key components of RF front-ends. With the continuous evolution of broadband wireless access (WiMAX), wireless local area networks (WLAN, such as IEEE 802.11a/b/g/n/ac/ax standards), and 6G technologies, demanding for filter performance has become increasingly stringent. These systems not only require filters to provide efficient and stable signal transmission across multiple passbands [1, 2], but also need to be miniaturized, in low power, and highly integrated to meet increasingly compact design requirements of communication devices.

Traditional dual-passband filter designs [3] often face challenges such as large size, difficulty in optimizing performance, and mutual interference between passbands. Although conventional step impedance resonator (SIR) [4–6] filters can generate a second passband through higher-order harmonics, correlation between the first and second passbands is high. Adjusting one band often causes changes in the other, making design process complex and difficult to achieve ideal performance. Additionally, with continuous expansion of communication passbands, there are higher demands for filter stopband rejection to ensure that the system is free from external interference signals. Recently, researchers have made significant progress in the design of dual-passband filters [7–9]. On one hand, by improving traditional dual-passband coupling schemes [10], various new structures [11, 12] have been proposed. Dual-passband filters with wide stopbands [13] based on hybrid microstrip/defected ground structures not only provide high-selectivity filtering effects in two bands but also feature ultra-wide stopbands [14] and low in-band insertion loss [15], effectively enhancing overall system performance. On the other hand, advanced design concepts using dual-mode resonators [16, 17] have enabled independent tuning capabilities for dual-passband filters, making design more flexible and better suited to meet complex and changing communication requirements [18, 19].

In this paper, a single SIR resonator load-coupled line is used for design [20, 21]. By bending SIR resonator to reduce overall size, this filter has two passbands located at 2.5 GHz and 5.5 GHz. Additionally, this filter forms four transmission zeros by loading coupled open stub lines, achieving good isolation between the two passbands.

2. THEORETICAL ANALYSIS

The lossless transmission line model of filter is shown in Figure 1. It uses a transmission line with characteristic impedances Z_{ce} and Z_{co} in series with a SIR stub line with characteristic impedance Z_2 for signal transmission. To enhance coupling, interdigital coupling is used for feeding, which also serves as part of coupled open stub lines. Inside resonator, a pair of open stub lines with characteristic impedance Z_3 is added to form coupling. The electrical lengths of all transmission lines are considered to be $\theta = \pi/2$.

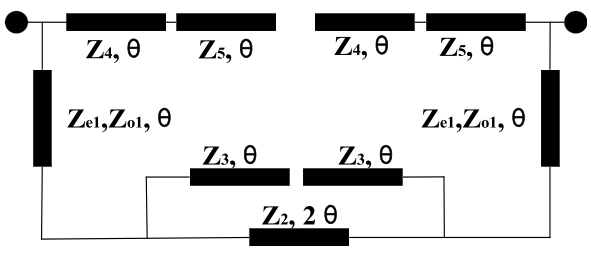

FIGURE 1. Lossless transmission line model.

* Corresponding author: Chuicai Rong (rongchuicai519@gnnu.edu.cn).

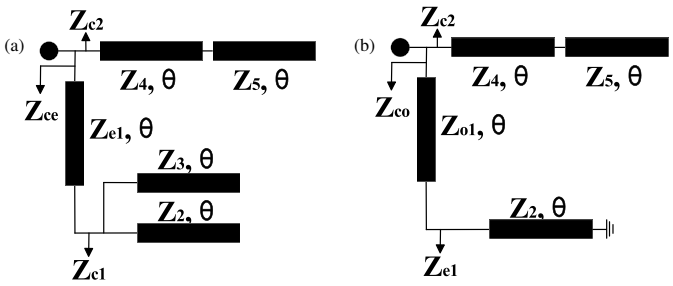

FIGURE 2. (a) Even-mode transmission line. (b) Odd-mode transmission line.

Due to the symmetry of circuit, even-odd mode analysis method is used. The equivalent circuits for odd mode and even mode are shown in Figures 2(a) and (b), respectively. The odd-mode impedance and even-mode impedance are derived as follows [22]:

$$Z_{odd} = \frac{Z_{co}Z_{c2}}{Z_{co}+Z_{c2}} \tag{1}$$

$$Z_{even} = \frac{Z_{ce}Z_{c2}}{Z_{ce}+Z_{c2}} \tag{2}$$

where:

$$Z_{co} = Z_{o1}\frac{Z_{e1}+jZ_{o1}\tan\theta}{Z_{o1}+jZ_{e1}\tan\theta} \tag{3}$$

$$Z_{e1} = jZ_2\tan\theta \tag{4}$$

$$Z_{ce} = Z_1\frac{Z_{c1}+jZ_{e1}\cot\theta}{Z_{e1}+jZ_{c1}\cot\theta} \tag{5}$$

$$Z_{c1} = -j\frac{Z_2Z_3\cot\theta}{Z_2+Z_3} \tag{6}$$

$$Z_{C2} = -jZ_4\frac{Z_4\tan\theta-Z_5\cot\theta}{Z_4+Z_5} \tag{7}$$

From Equations (1) and (2), even-mode admittance and odd-mode admittance can be obtained. The S-parameters of filter can be expressed as:

$$S_{11} = \frac{Y_0^2-Y_{even}Y_{odd}}{(Y_0+Y_{even})(Y_0+Y_{odd})} \tag{8}$$

$$S_{21} = \frac{Y_0(Y_{even}-Y_{odd})}{(Y_0+Y_{even})(Y_0+Y_{odd})} \tag{9}$$

By substituting Equations (1) and (2) into Equation (8), transmission zero of filter can be obtained by $|S_{21}|=0$, that is:

$$Z_{c2}(Z_{ce}-Z_{co}=0) \tag{10}$$

When $Z_{c2}=0$, following can be obtained:

$$\theta = \cot^{-1}\sqrt{\frac{Z_4}{Z_5}} \tag{11}$$

When $(Z_{ce}-Z_{co}=0)$, following can be obtained:

$$\theta = \tan^{-1}\sqrt{\frac{-Z_{e1}Z_{c1}}{Z_{e1}Z_{o1}+Z_{c1}Z_{o1}-Z_{e1}^2}} \tag{12}$$

According to the relationship between electrical length and design frequency, transmission zero (TZ) frequency can be determined using formula (11):

$$f_{TZn} = \frac{\theta_{TZn}}{\theta_0}f_0\,(n=3,4) \tag{13}$$

From Equations (10) to (12), f_{TZ1} and f_{TZ2} can be calculated. Since the response is symmetric, f_{TZ3} and f_{TZ4} can be obtained from $2f_0-f_{TZ1}$ and $2f_0-f_{TZ2}$, respectively. Considering that $Z_{e1}=65.4\,\Omega$, $Z_{o1}=38.3\,\Omega$, $Z_1=50\,\Omega$, $Z_2=74.0\,\Omega$, $Z_3=Z_5=116\,\Omega$, $Z_4=74.2\,\Omega$, and $\theta=90°$, $f_0=5.5$ GHz, the transmission zeros can be calculated to be 3.5 GHz, 5.0 GHz, 6 GHz, 7 GHz, and all zeros are symmetric about 5.5 GHz.

3. DESIGN AND SIMULATION

Based on the generalized Chebyshev theory, a dual-passband filter operating at 2.5 GHz and 5.5 GHz is designed. The structure of the designed dual-passband filter is shown in Figure 3(a), and simulation results of the filter are shown in Figure 3(b).

Based on theory mentioned above, considering the impact of the sizes of Z_3, Z_4, and Z_5 on coupled open stubs, simulation software is used to simulate and obtain the optimal values. The simulation results are shown in the Figures 4(a), (b), and (c).

As shown in Figure 4, variations in Z_3 and Z_5 significantly impact the bandwidth and insertion loss of the second passband. With an increase in Z_3, the center frequency of the second passband shifts toward lower frequencies, accompanied by the relocation of transmission zeros f_{TZ3} and f_{TZ4}. Similarly, as Z_5 increases, the bandwidth of the second passband decreases, while transmission zeros f_{TZ1} and f_{TZ2} are shifted. In contrast, Z_4 primarily affects the return loss of both passbands.

The values are determined based on different response situations. Finally, overall EM simulation of this filter using HFSS and the dimensions of parameters are optimized and determined through simulation. The specific dimensions are as follows: $W_1=1.56$ mm, $W_2=0.80$ mm, $W_3=0.30$ mm, $W_4=0.30$ mm, $W_5=1.56$ mm, $L_1=11.00$ mm, $L_2=15.21$ mm, $L_3=4.00$ mm, $L_4=5.00$ mm, $L_5=5.00$ mm, $L_6=5.00$ mm, $L_7=6.00$ mm, $L_8=3.44$ mm, $L_9=3.00$ mm.

4. FABRICATION AND MEASUREMENTS

The dual-passband filter was measured using a vector network analyzer, Agilent E5222A. Figure 5 shows the comparison between simulated and measured results of filter.

From Figure 5, it can be seen that center frequency of low passband is 2.53 GHz, with a 3.0 dB bandwidth range of $2.48\sim2.57$ GHz. The group delay within the first passband ranges from 0.63 ns to 4.35 ns, with a minimum insertion loss of 1.13 dB and a return loss of 18.60 dB. The center frequency

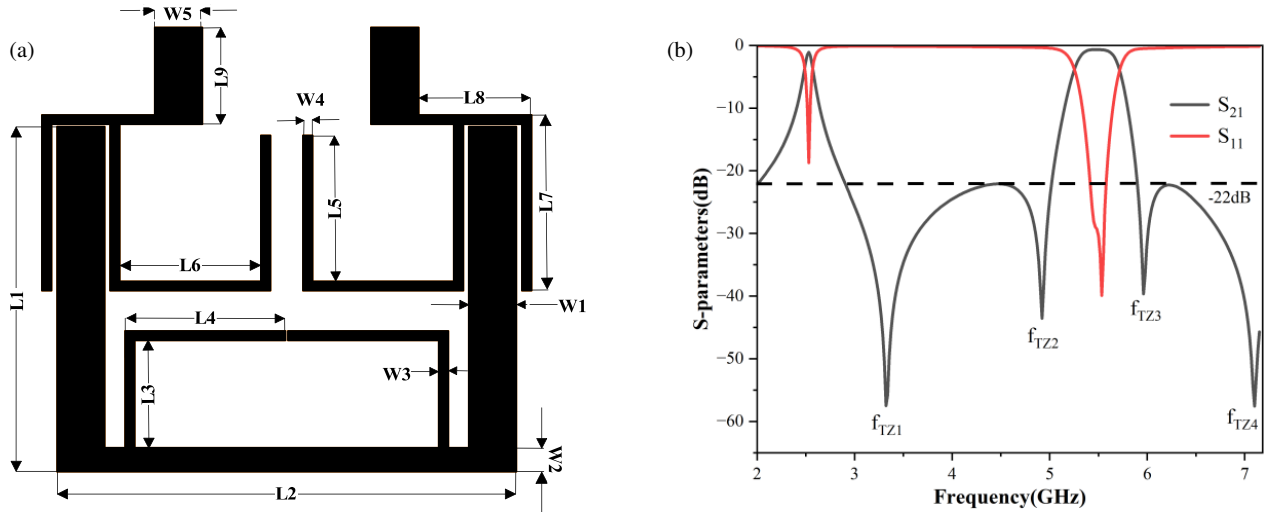

FIGURE 3. (a) Electromagnetic simulation model of filter. (b) Simulation S-parameters of filter.

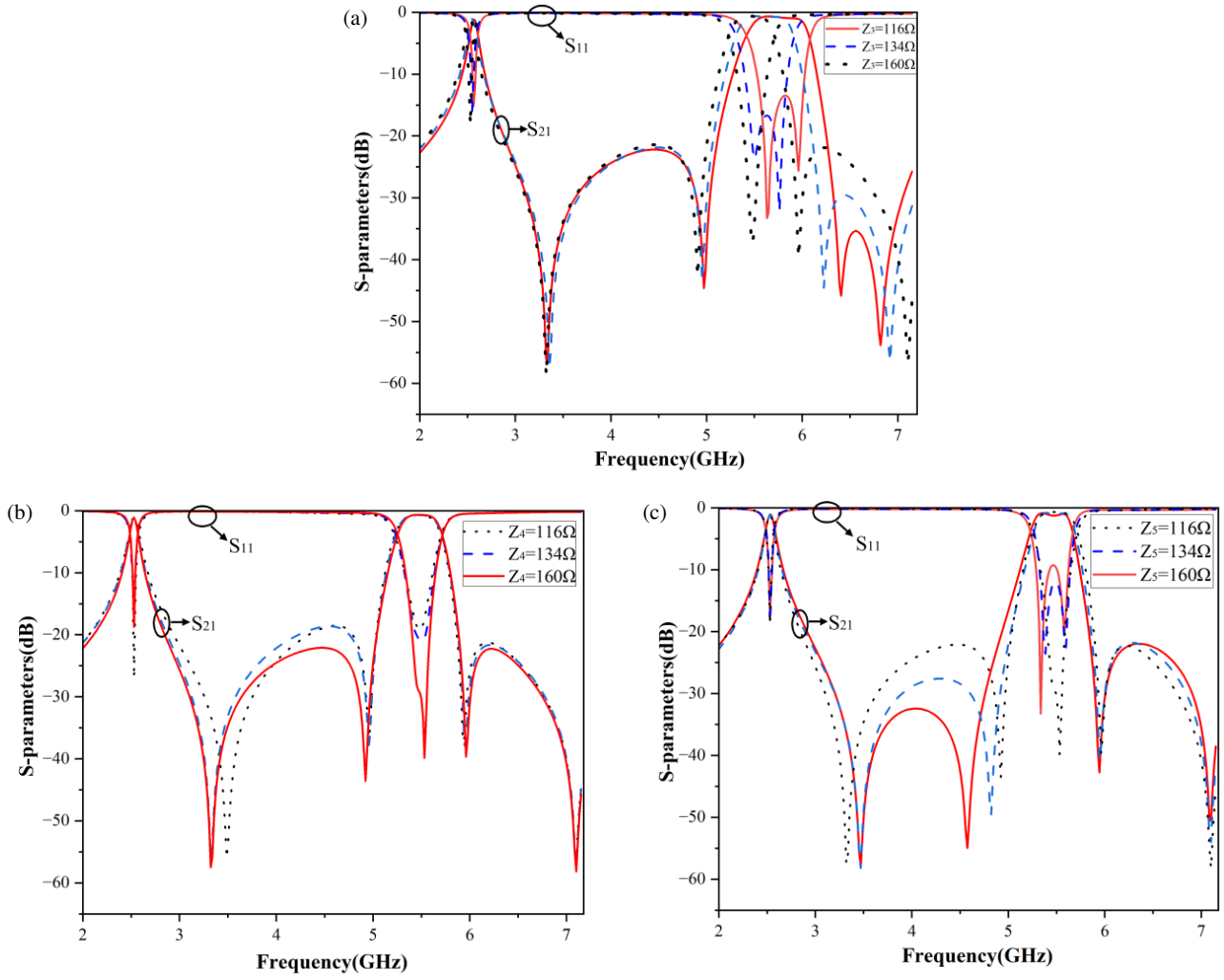

FIGURE 4. (a) Simulation results of different Z_3. (b) Simulation results of different Z_4. (c) Simulation results of Z_5.

of high passband is 5.53 GHz, with a 3.0 dB bandwidth range of $5.23 \sim 5.75$ GHz. The group delay within the second passband ranges from 1.32 ns to 2.00 ns, with a minimum insertion loss of 0.70 dB and a return loss of 22.89 dB. Using coupled open stub lines, four transmission zeros are introduced outside passbands at 3.29 GHz, 4.94 GHz, 5.96 GHz, and 7.10 GHz with all four zeros symmetrically distributed around 5.5 GHz. The main reason for inconsistency between measured results and simulated

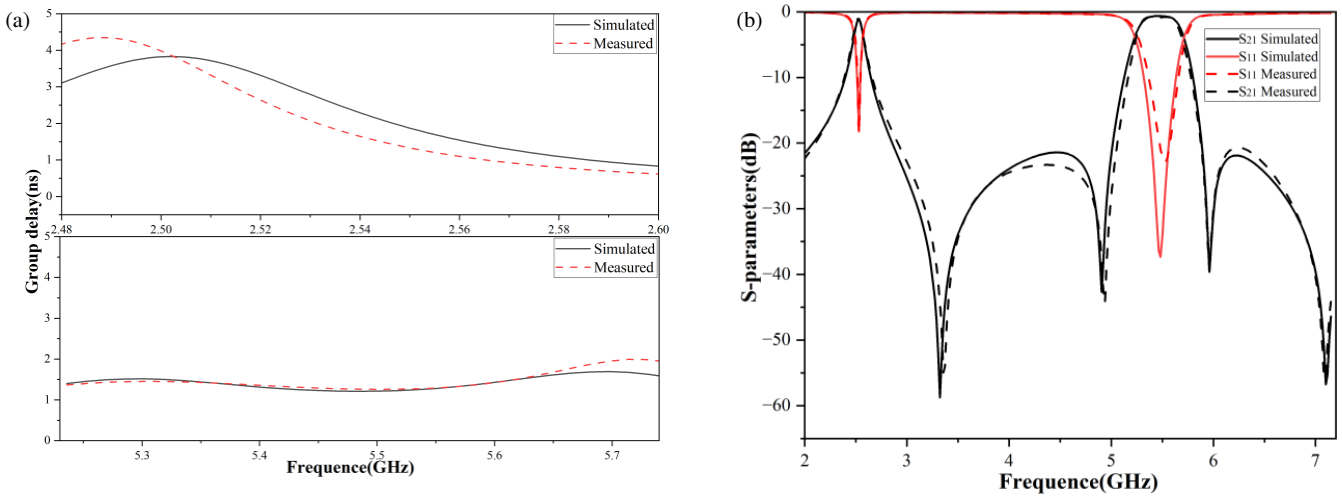

FIGURE 5. (a) Comparison of simulated and measured group delays of filter. (b) Comparison of simulated and measured S-parameters of filter.

TABLE 1. Comparison with published filters.

Ref.	f_0 (GHz)	Size (λ_g^2)	FBW (%)	IL[1] (dB)	RL[2] (dB)	No. of TZs[3]
[6]	2.45/5.60	0.057	none	2.8/2.9	17.0/21.0	none
[18]	2.60/5.80	0.0884	14.3/10.7	1.3/2.8	20.0/21.0	3
[20]	2.40/5.20	0.056	51.9/22.3	0.3/0.7	22.1/20.8	3
[23]	2.40/5.20	0.060	28.0/15.0	0.1/0.9	18.2/16.7	1
[24]	0.35/0.95	0.011	11.2/9.5	1.4/1.1	20.0/18.0	3
This work	2.5/5.53	0.046	3.0/9.5	1.1/0.7	18.6/22.9	4

[1] Insertion Loss [2] Return Loss [3] Number of Transmission Zeros

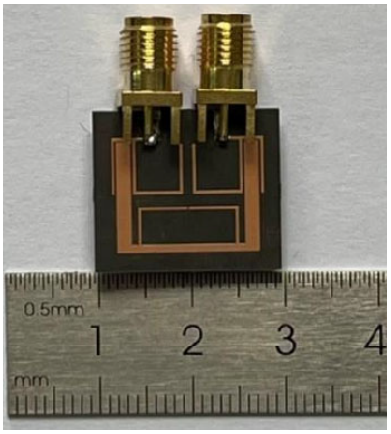

FIGURE 6. Photograph of fabricated filter.

results is that nonuniform solder affects the passband performance at high frequency during SMA joint welding.

The optimized parameter dimensions are used to manufacture filter. The substrate used for processing is Rogers RT/Duroid5880. The dielectric constant is 2.20. The loss tangent angle δ is 0.0009, and the thickness is 0.508 mm. The resulting filter dimensions are $20\lambda_g \times 0.23\lambda_g$, where λ_g corresponds to wavelength at the center frequency (2.50 GHz) of the first passband. The physical diagram of filter is shown in Figure 6. Table 1 compares the performance of this filter with other filters in published papers.

5. CONCLUSION

This paper proposes a U-shaped resonator structure loaded with coupled open stub lines. The loaded-coupled open stub lines create four transmission zeros outside passband, with four zeros symmetrically distributed around 5.5 GHz. Based on the theory of lossless transmission lines and even-odd mode analysis, the reasons for the formation of transmission zeros in filters are analyzed. The proposed filter has a compact size, high isolation between the passbands, and good selectivity.

ACKNOWLEDGEMENT

This work was supported by science and technology project of Jiangxi Provincial Department of Education (GJJ2201211), Key Research and Development Plan of Ganzhou (2022BGY9645), Ministry of Education Industry-University Cooperative Education Project (241005789141509), Innovation and Entrepreneurship Training Program for college students (S202410418017).

REFERENCES

[1] Shankar, E., K. V. P. Kumar, and V. K. Velidi, "Design of high selectivity compact dual-band bandpass filter with seven transmission-zeros for GPS and WiMAX applications," *IEEE Transactions on Circuits and Systems II: Express Briefs*, Vol. 70, No. 7, 2395–2399, 2023.

[2] Arif, K., K. V. P. Kumar, R. K. Barik, and G. Chakaravarthi, "A planar quad-band bandpass filter employing transmission lines loaded with tri-stepped impedance open- and dual-stepped impedance short-ended resonators," *Progress In Electromagnetics Research C*, Vol. 147, 65–72, 2024.

[3] He, M., X. Zuo, H. Mei, and Y. Li, "A planar five-section short-length coupled-line band-stop filter with two reconfigured states," *Progress In Electromagnetics Research C*, Vol. 147, 161–166, 2024.

[4] Iqbal, A., J. J. Tiang, S. K. Wong, S. W. Wong, and N. K. Mallat, "QMSIW-based single and triple band bandpass filters," *IEEE Transactions on Circuits and Systems II: Express Briefs*, Vol. 68, No. 7, 2443–2447, 2021.

[5] Verdú, J., E. Guerrero, L. Acosta, and P. de Paco, "Exact synthesis of inline fully canonical dual-band filters using dual extracted-pole sections," *IEEE Microwave and Wireless Components Letters*, Vol. 31, No. 12, 1255–1258, 2021.

[6] Fernández-Prieto, A., J. Martel, P. J. Ugarte-Parrado, A. Lujambio, A. J. Martinez-Ros, F. Martín, F. Medina, and R. R. Boix, "Compact balanced dual-band bandpass filter with magnetically coupled embedded resonators," *IET Microwaves, Antennas & Propagation*, Vol. 13, No. 4, 492–497, 2019.

[7] Zhao, X.-B., F. Wei, P. F. Zhang, and X. W. Shi, "Mixed-mode magic-Ts and their applications on the designs of dual-band balanced out-of-phase filtering power dividers," *IEEE Transactions on Microwave Theory and Techniques*, Vol. 71, No. 9, 3896–3905, 2023.

[8] Wei, F., B. Liu, Z. Li, L. Xu, R. Li, Y. Yang, and X. N. Yang, "Balanced dual-band BPF and FPD using quad-mode RLR with improved selectivity," *IEEE Transactions on Circuits and Systems II: Express Briefs*, Vol. 69, No. 4, 2081–2085, 2022.

[9] Zhao, X.-B., F. Wei, L. Yang, and R. Gómez-García, "Two-layer-magic-T-based bandpass, quasi-bandstop, and dual-passband balanced filters with differential-/common-mode reflectionless behavior," *IEEE Transactions on Microwave Theory and Techniques*, Vol. 72, No. 4, 2267–2282, 2024.

[10] Killamsetty, V. K. and B. Mukherjee, "Miniaturised highly selective wide-band bandpass filter using dual-mode resonators and inter digital capacitors," *Electronics Letters*, Vol. 53, No. 17, 1209–1211, 2017.

[11] Kumar, K. V. P., V. K. Velidi, A. A. Althuwayb, and T. R. Rao, "Microstrip dual-band bandpass filter with wide bandwidth using paper substrate," *IEEE Microwave and Wireless Components Letters*, Vol. 31, No. 7, 833–836, 2021.

[12] Li, D., M.-C. Tang, Y. Wang, K.-Z. Hu, and R. W. Ziolkowski, "Dual-band, differentially-fed filtenna with wide bandwidth, high selectivity, and low cross-polarization," *IEEE Transactions on Antennas and Propagation*, Vol. 70, No. 6, 4872–4877, 2022.

[13] Li, D. and K.-D. Xu, "Multifunctional switchable filter using coupled-line structure," *IEEE Microwave and Wireless Components Letters*, Vol. 31, No. 5, 457–460, 2021.

[14] Lin, W., K. Zhou, and K. Wu, "Band-reconfigurable tunable bandpass filters based on mode-switching concept," *IEEE Transactions on Microwave Theory and Techniques*, Vol. 71, No. 3, 1125–1135, 2022.

[15] Gómez-García, R., L. Yang, J.-M. Muñoz-Ferreras, and D. Psychogiou, "Selectivity-enhancement technique for stepped-impedance-resonator dual-passband filters," *IEEE Microwave and Wireless Components Letters*, Vol. 29, No. 7, 453–455, 2019.

[16] Liu, B.-G., Y.-P. Lyu, L. Zhu, and C.-H. Cheng, "Compact single- and dual-band filters on hexa-modes half-mode substrate integrated waveguide resonator with loaded H-shaped slot," *IEEE Microwave and Wireless Components Letters*, Vol. 30, No. 12, 1129–1132, 2020.

[17] Zhang, Q., C. Chen, W. Chen, J. Ding, and H. Zhang, "Novel cross-coupled dual-band bandpass filters with compact size based on dual-mode isosceles right-angled triangular resonators," *IEEE Transactions on Microwave Theory and Techniques*, Vol. 69, No. 6, 3037–3047, 2021.

[18] Liu, B.-G., Y.-P. Lyu, L. Zhu, and C.-H. Cheng, "Compact single- and dual-band filters on hexa-modes half-mode substrate integrated waveguide resonator with loaded H-shaped slot," *IEEE Microwave and Wireless Components Letters*, Vol. 30, No. 12, 1129–1132, 2020.

[19] He, M., X. Zuo, H. Mei, and Y. Li, "A planar five-section short-length coupled-line band-stop filter with two reconfigured states," *Progress In Electromagnetics Research C*, Vol. 147, 161–166, 2024.

[20] Liang, G.-Z. and F.-C. Chen, "A compact dual-wideband bandpass filter based on open-/short-circuited stubs," *IEEE Access*, Vol. 8, 20 488–20 492, 2020.

[21] Xie, H.-W., K. Zhou, C.-X. Zhou, and W. Wu, "Analysis of four-stage stepped-impedance resonators and their application to quad-band microstrip bandpass filter," *International Journal of RF and Microwave Computer-Aided Engineering*, Vol. 30, No. 4, e22116, 2020.

[22] Pozar, D. M., *Microwave Engineering: Theory and Techniques*, 4th ed., John Wiley & Sons, Hoboken, NJ, 2021.

[23] Salmani, R., A. Bijari, and S. H. Zahiri, "A compact dual-band bandpass filter using coupled microstrip lines," *IETE Journal of Research*, Vol. 69, No. 12, 8554–8560, 2023.

[24] Killamsetty, V. K. and B. Mukherjee, "Compact dual bandpass filter for terrestrial radio and GSM applications," *International Journal of RF and Microwave Computer-Aided Engineering*, Vol. 27, No. 8, e21131, 2017.